



High-Temperature Oxidation and Hot Corrosion Behavior of Two Kinds of Thermal Barrier Coating Systems for Advanced Gas Turbines

M. Yoshida, K. Abe, T. Aranami, and Y. Harada

High-temperature oxidation and hot corrosion tests were conducted at 800 to 1100 °C under isothermal and thermal-cycle conditions for two kinds of thermal barrier coating (TBC) systems with different compositions of ceramic top coat: Y₂O₃-stabilized zirconia (YSZ) and CaO-SiO₂-ZrO₂ (C₂S-CZ). Qualitative and quantitative failure analyses were carried out to clarify the failure mechanisms of TBC systems.

In high-temperature oxidation up to 1100 °C, the YSZ-TBC system was subjected more easily to spalling of the ceramic top coat. This is attributed to the localized oxidation along the ceramic top coat/metallic (NiCrAlY) bond coat interface, as compared with the case of the C₂S-CZ-TBC system. Thus, the most significant oxidation damage resulted in the YSZ system under the thermal-cycle condition. On the other hand, for hot corrosion by Na₂SO₄-NaCl molten salt up to 1000 °C, the C₂S-CZ system was more reactive with the molten salt to form a new phase layer composed of both the metallic bond coat constituents, such as aluminum and chromium, and corrosive species such as oxygen at the inner region of the ceramic top coat. Furthermore, effects of both the heat treatment, in particular the atmosphere after plasma spraying, and the chromium content of the bond coat were investigated for each coating system.

Keywords ceramic coating, failure analysis, high-temperature oxidation, hot corrosion, thermal barrier coating system

1. Introduction

AN INCREASING demand for higher-strength properties and better corrosion resistance for nickel-base superalloys for advanced gas turbines has created the need for a protective coating to improve reliability (Ref 1). Among many kinds of coating technologies, plasma spraying is expected to be most promising for high-performance coating systems at temperatures up to ~1100 °C (Ref 2). Therefore a number of property evaluation

M. Yoshida, Department of Precision Engineering, Tokyo Metropolitan University, Minami-Osawa 1-1, Hachioji, Tokyo 192-03, Japan; K. Abe, Graduate School, Tokyo Metropolitan University, Tokyo 192-03, Japan; T. Aranami, Graduate School, Tokyo Metropolitan University (presently at IHI, Tokyo 135, Japan); and Y. Harada, Thermal Spraying Technology R&D Laboratory, Tocalo Co., Ltd., Higashi-Nada, Kobe 658, Japan.

studies have been made from different aspects: from characterization of the coating films formed to practical property evaluations such as evaluation of oxidation resistance (Ref 3) and development of plasma processing (Ref 4). However, the failure mechanism of advanced thermal barrier coating (TBC) systems under thermochemical loading conditions remains unclear in spite of its practical significance (Ref 5).

In the present study, both high-temperature oxidation and hot corrosion behavior under isothermal and thermal-cycle conditions were investigated for two kinds of TBC systems with different compositions of ceramic top coat. One TBC system is a conventional Y₂O₃-stabilized ZrO₂ (YSZ), which is used in gas turbine applications such as combustion cans and stator vanes. The other is the CaO-SiO₂-ZrO₂ (C₂S-CZ), in which there are many microcracks that are beneficial for mitigating thermal shock in the ceramic top coat layer. The purpose of this study is to clarify the degradation behavior and failure mechanism of the TBC systems under different thermochemical loadings.

Table 1 Processing condition of various TBC systems

Symbol	Heat treatment(a)	Sand blast	Metallic bond coat, thickness 100 μm	Ceramic top coat, thickness 200 μm	Heat treatment(b)
BX	Yes	No	No
ZV	Yes	Yes	VPS-NiCrAlY (L)	APS-YSZ	Yes (Vac.)
ZA	Yes	Yes	VPS-NiCrAlY (L)	APS-YSZ	Yes (Air)
SV	Yes	Yes	VPS-NiCrAlY (L)	APS-C ₂ S-CZ	Yes (Vac.)
SA	Yes	Yes	VPS-NiCrAlY (L)	APS-C ₂ S-CZ	Yes (Air)
SC	Yes	Yes	VPS-NiCrAlY (L)	APS-C ₂ S-CZ	No
HZV	Yes	Yes	VPS-NiCrAlY (H)	APS-YSZ	Yes (Vac.)
HSV	Yes	Yes	VPS-NiCrAlY (H)	APS-C ₂ S-CZ	Yes (Vac.)
HSA	Yes	Yes	VPS-NiCrAlY (H)	APS-C ₂ S-CZ	Yes (Air)
HSC	Yes	Yes	VPS-NiCrAlY (H)	APS-C ₂ S-CZ	No

(a) THT: 1180 °C × 2 h → AC + 850 °C × 24 h → AC + 750 °C × 20 h → AC. (b) (Vac.), solution treatment in vacuum; (Air), solution treatment in air

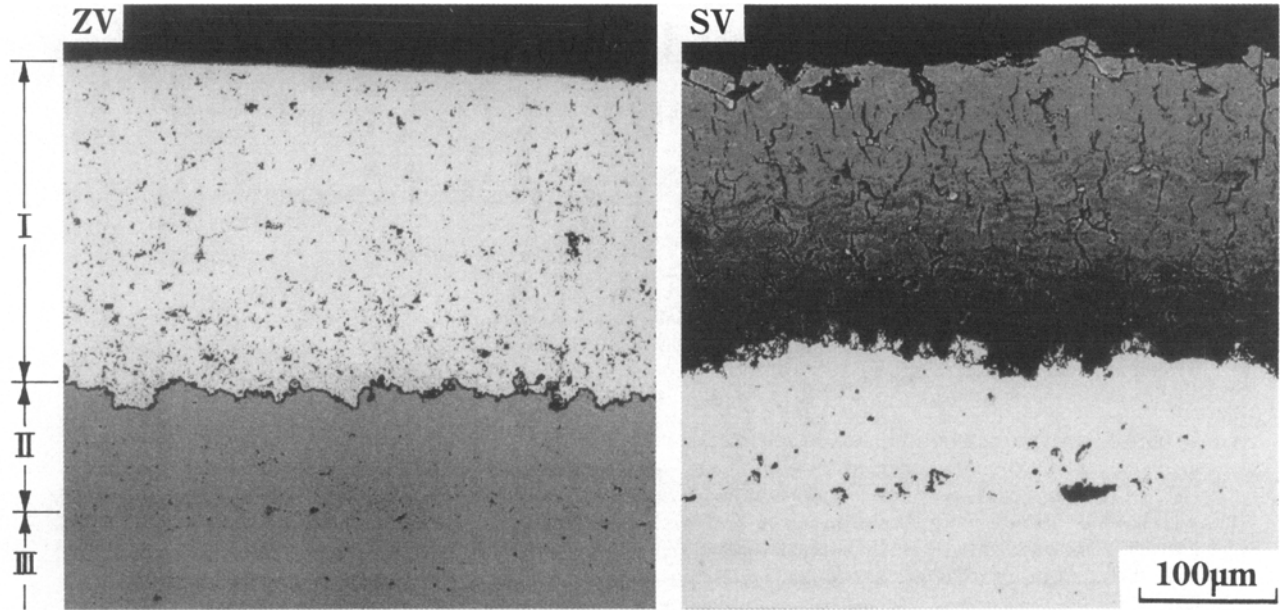


Fig. 1 Typical cross-sectional microstructures by backscattered electron image for the ZV and SV specimens after the heat treatment. I. APS top coat; II, VPS bond coat; III, alloy substrate. The process codes ZV and SV are defined in Table 2.

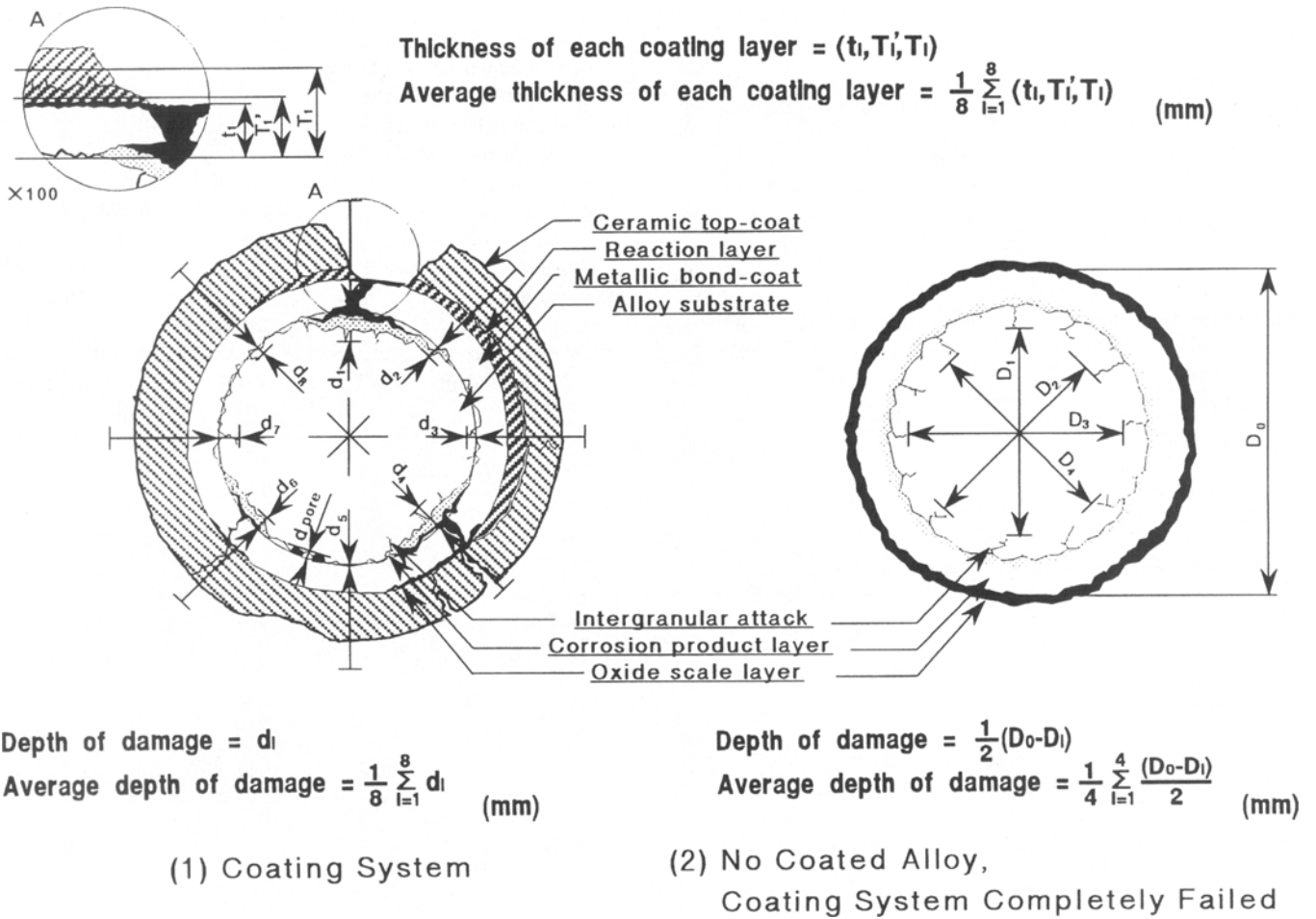


Fig. 2 Schematic illustration for both the failure morphologies observed in the present tests and the evaluation methodology for the damage depth

2. Experimental Procedures

Two kinds of TBC systems composed of the ceramic top coat/metallic bond coat/nickel-base superalloy substrate were adopted in this study. The nickel-base alloy substrate is Inconel X750, which has a chemical composition of (mass%): 0.04 C, 0.31 Si, 0.20 Mn, 0.002 S, 15.85 Cr, 2.36 Ti, 0.80 Al, 7.50 Fe, 0.16 Cu, 1.01 Nb + Ta, bal Ni. TBC systems and their processing conditions are summarized in Table 1, and the compositions of the feedstock powders are listed in Table 2. Plasma spraying of the metallic bond coat and ceramic top coat were carried out in a low-pressure argon atmosphere (VPS) and in air (APS), respectively, onto the cylindrical surface of specimens of 13 mm in diameter and 10 mm in thickness. The specimen thickness 10 mm was determined on the basis of prior hot corrosion tests to be sufficient for a reliable coating failure analysis, by minimizing the edge and/or corner effect of the corrosive damage. The details of plasma spraying conditions are shown in Table 3. Heat treatments of the sprayed specimens were carried out either in vacuum or in air, according to the specification (triple heat treatment, THT) for the alloy substrate. As a typical example, the cross-sectional microstructures of ZV and SV specimens after heat treatment are shown in Fig. 1. The process codes ZV and SV are defined in Table 1.

High-temperature oxidation tests were carried out at 1000 and 1100 °C up to 100 h in static air under isothermal or thermal cycle (10 h cyclic) conditions, using a conventional electric furnace. On the other hand, hot corrosion tests were conducted at 800 to 1000 °C up to 100 h by applying a synthetic salt mixture composed of 90% Na₂SO₄ and 10% NaCl (melting point 785 °C) onto the surface of TBC specimens of the same dimensions as those used in the oxidation test. The quantity of the salt coated was controlled in the isothermal and thermal cycle tests to 40 mg/cm² and 20 mg/cm², respectively (Ref 6, 7). In the thermal cycle test, the same amount of salt was repeatedly supplied at every cooling chance. For a reproducibility check, both high-temperature oxidation and hot corrosion tests were carried out using more than two specimens under the same conditions.

After the tests, all the specimens were cross sectioned and metallographically examined. Various types of failure morphologies observed in this study are schematically illustrated in

Table 2 Constituents of coating layer (mass %)

Layer	Code	Composition, %
Bond coat	NiCrAlY (L)	Ni-17Cr-5Al-0.5Y
	NiCrAlY (H)	Ni-23Cr-6Al-0.5Y
Top coat	YSZ	ZrO ₂ -6%Y ₂ O ₃
	C ₂ S-CZ	2CaO · SiO ₂ -15%CaO · ZrO ₂

Table 3 Plasma spraying condition in VPS and APS

Item	VPS	APS
Spray system	Plasma Technik A-2000V	Plasma Technik A-3000S
Power	37 kW	48 kW
Plasma gas	Ar/H ₂	Ar/H ₂
Atmosphere	70 mbar in Ar	Air
Spray distance	275 mm	120 mm

Fig. 2. A metallographic measurement was then made to determine the depth of damage from the bond coat/alloy substrate interface into the alloy substrate (Ref 8). An average thickness of residual coating layer that maintains coating-substrate adhesion was also measured as an index of the spallation resistance. Various analytical techniques were used for the failure analysis, such as scanning electron microscopy with energy dispersive x-ray spectroscopy (SEM-EDX), electron probe x-ray microanalysis (EPMA), and x-ray diffraction analysis (XRD).

3. Results

3.1 High-Temperature Oxidation of TBC Systems

In this section, the results of oxidation tests at only 1100 °C will be detailed, because at 1000 °C little difference was observed among various coating systems.

3.1.1 Oxidation Behavior

The high-temperature oxidation kinetics at 1100 °C for the different TBC systems are shown in Fig. 3 in terms of the damage depth. Here, a scatter band in the damage depth represents the data scatter among the different sections measured. The oxi-

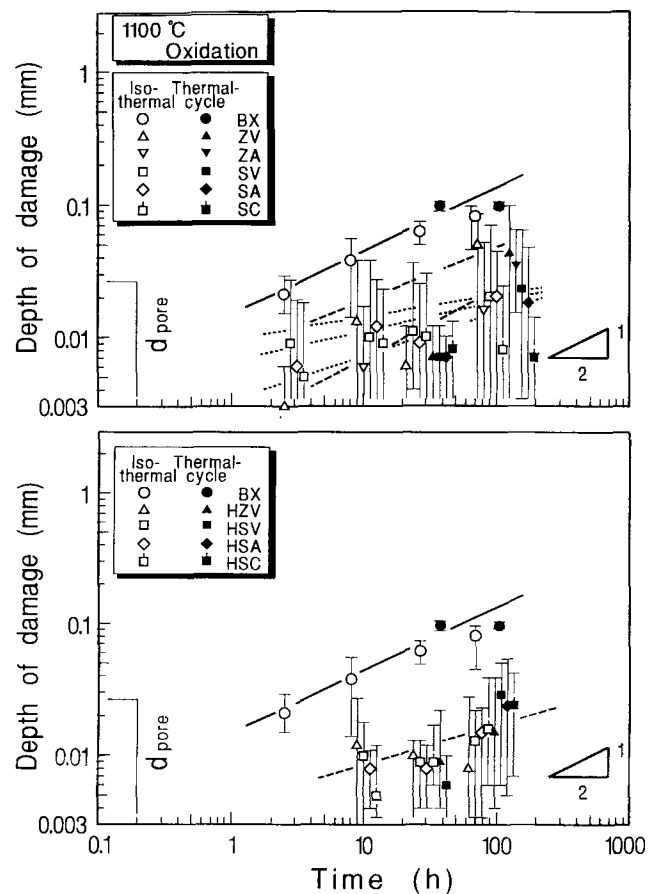


Fig. 3 High-temperature oxidation kinetics in terms of the damage depth for different TBC systems at 1100 °C for 100 h under isothermal and thermal cycle conditions

dation kinetics of the uncoated Inconel X750 (BX) follows a parabolic rate law, suggesting that the inward oxidation, which takes the form of grain boundary oxidation, is diffusion controlled. On the other hand, all the TBC systems show a much smaller average damage depth than the Inconel X750 (BX), with a size less than that of an initial defect, d_{pore} which probably was introduced during the sand-blasting process. However, localized oxidation damage tends to occur in the TBC systems to the same damage depth in the maximum as in the uncoated BX sample, as shown by the very large data scatter from section to section. In particular, the data scatter is more pronounced in the TBC systems with the low Cr-NiCrAlY bond coat (i.e., samples ZV, ZA, SV, SA, and SC).

Figure 4 shows the damage depth together with an average thickness of the residual coating layer after the 100 h oxidation test at 1100 °C. Again, all the TBC systems are found to result in improved resistance against oxidation damage, because the average damage depth is markedly reduced for all the TBC systems compared to the uncoated Inconel X750 (BX).

For the YSZ-TBC systems, the heat treatment in air brings about reduced oxidation of the alloy substrate under the isothermal conditions, because ZA shows a substantially decreased damage depth compared to ZV. This is attributed to the protective effect of the oxide film at the top coat/bond coat interface, which was developed in the heat treatment process in air. However, thermal cycle oxidation tends to exacerbate the damage to an alloy substrate, which is induced by the premature spalling of

the YSZ top coat. Regarding the effect of chromium content in the NiCrAlY bond coat, an increase in chromium content suppresses oxidation damage of the alloy substrate, although the resistance against the top coat spalling is hardly improved.

For the C₂S-CZ-TBC system, on the other hand, little difference in damage depth was observed among various C₂S-CZ systems, except for SC which was subjected to no heat treatment. Such low damage for SC specimen suggests that eliminating the heat treatment will bring about an improved oxidation resistance.

The oxidation behavior of the C₂S-CZ-TBC system is characterized by a new phase layer developed at the inner region of the ceramic top coat layer, which will be termed a reaction layer. Characterization of the reaction layer is discussed below. Thus, such a reaction layer seems beneficial for improving adhesion between the bond coat and top coat, because substantial thickness of the top coat is retained in both SV and SA, even under conditions of thermal cycle oxidation. Furthermore, no advantage of increasing the chromium content in the NiCrAlY bond coat was observed for the C₂S-CZ-TBC system, contrary to the case of the YSZ-TBC system.

3.1.2 Microstructural Features of Oxidation-Induced Failure

Figure 5 shows optical micrographs of different TBC systems after the 100 h isothermal and 10 h × 10 cyclic oxidation tests at 1100 °C. In the YSZ-TBC system, a number of cracks penetrate across the ceramic top coat layer, which appear to be

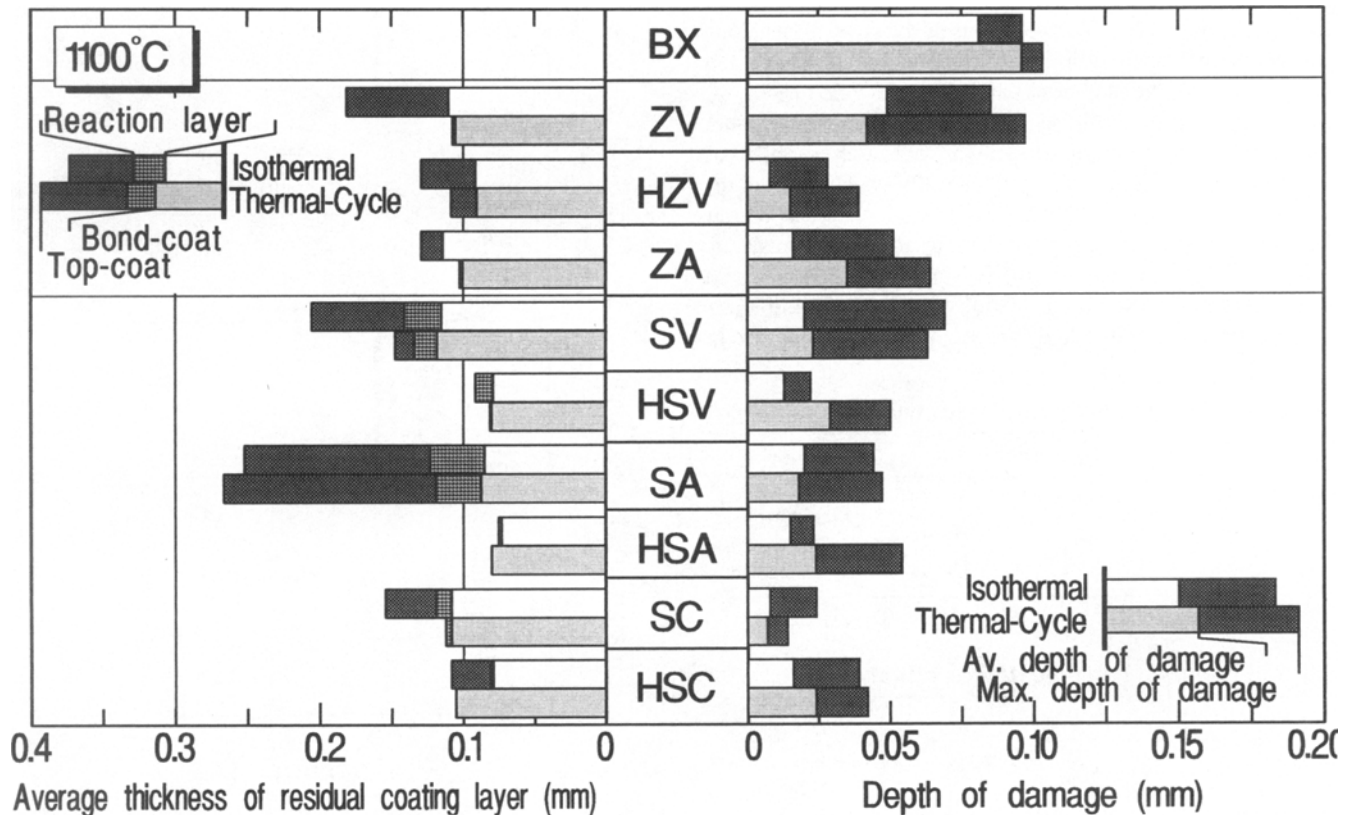


Fig. 4 Average thickness of residual coating layer and the damage depth for different TBC systems after the oxidation test at 1100 °C for 100 h under isothermal and thermal cycle conditions

introduced during the spraying and/or heat treatment processes. Such a penetrating crack induces preferential oxidation along the top coat/bond coat interface and eventually causes extensive spalling of the top coat. Thus, an oxidation-induced top coat spalling should be more pronounced under the thermal cycle condition, as can be seen in Fig. 5. However, under thermal cycle oxidation up to 1100 °C, the alloy substrate is subjected to little oxidation damage, mainly due to good oxidation resistance of the NiCrAlY bond coat.

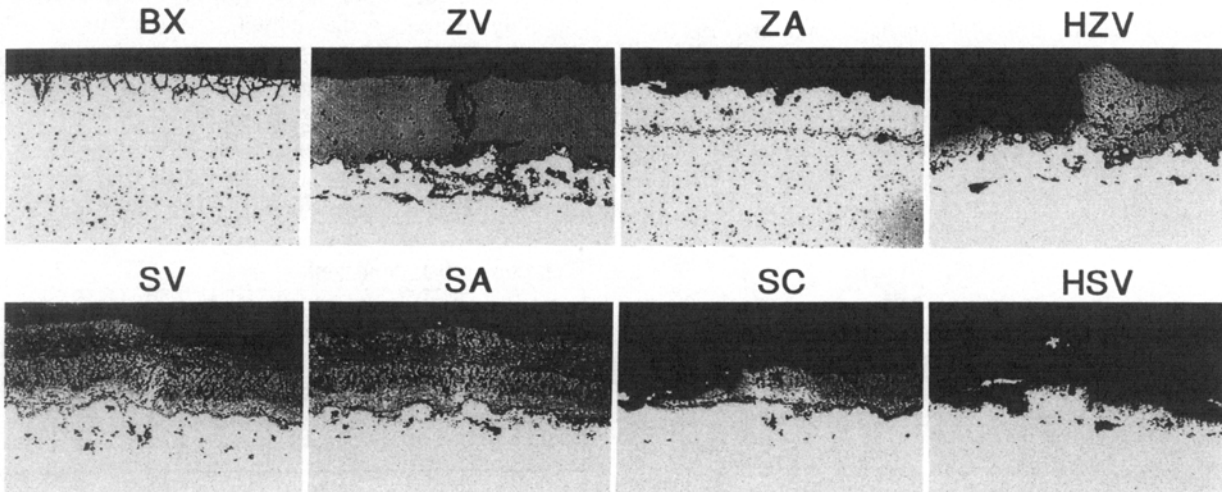
For the C₂S-CZ-TBC system, on the other hand, neither extensive exfoliation nor penetrating cracking takes place in the ceramic top coat, even under thermal cycle oxidation, provided that any heat treatment is employed. The SC sample without heat treatment, however, exhibits a relatively large amount of top coat spalling, probably because of its compositional and microstructural heterogeneity. The C₂S-CZ-TBC system with a high-chromium bond coat (HSV, HSA, and HSC) also was subjected to the top coat spalling, as can be seen for HSV in Fig. 5.

This may be attributed to poor adhesion between the top coat and bond coat, because of the development of a chromium-rich interfacial oxide.

Again, the oxidation morphology of the C₂S-CZ system is characterized by formation of a reaction layer. It has been revealed from SEM-EDX and EPMA analyses that this layer tends to develop at the expense of aluminum and/or chromium from the NiCrAlY bond coat. As mentioned below, the reaction layer is generally beneficial, not only as a protective barrier against inward oxidation toward the bond coat and alloy substrate, but also in enhancing adhesion between the top coat and bond coat.

Figure 6 shows a summarized characterization of the coating microstructure developed in the C₂S-CZ-TBC system, including typical micrographs and the corresponding illustration, EDX and Vickers microhardness (load 0.98 N) distributions. High-temperature oxidation brings two main kinds of microstructural changes in the ceramic top coat: the reaction layer formation and the appearance of the lamellar structure region

1100 °C – 100h Isothermal



1100 °C – 10h × 10cycle

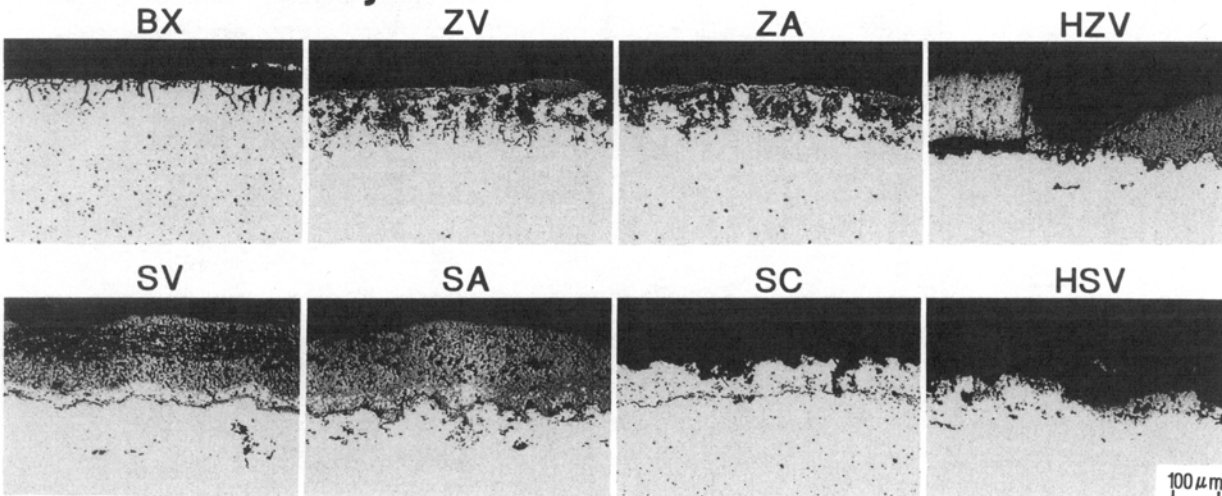


Fig. 5 Optical micrographs at the cross-sectional surface zone of different TBC systems after the oxidation test at 1100 °C for 100 h

in the midway to outer side of the top coat. The former is characterized by an increased hardness and a substantial amount of the bond coat constituents, such as aluminum, chromium, and/or partly nickel. This suggests that complex oxides composed of aluminum, chromium, and/or nickel were formed in this region, although they could not be detected by XRD. It was found that such a reaction layer is suppressed by increasing the chromium content in the bond coat, as shown in Fig. 4. For the latter, on the other hand, ceramic top coat is free of bond coat constituents and has a different Ca/Si ratio from the surroundings. It can be deduced, therefore, that some crystalline phases, probably of complex oxides, were formed by virtue of oxidation-induced transformations. In any case, the C₂S-CZ top coat appears to be highly reactive with the surrounding materials.

3.2 Hot Corrosion of TBC Systems

3.2.1 Hot Corrosion Behavior

Hot corrosion kinetics at 1000 °C for different TBC systems are shown in Fig. 7, in terms of the damage depth. All the TBC systems exhibit a much smaller damage depth than the uncoated Inconel X750 (BX), where the damage depth is the same as for high-temperature oxidation if isothermal oxidation is considered. However, thermal cycle corrosion brings about much greater damage corresponding to an almost linear rate law, for any TBC system.

Figure 8 is a summary of the damage depth together with an average thickness of residual coating layer for different TBC systems after the 100 h hot corrosion test at 800 to 1000 °C. At 800 °C, all the TBC systems show the significantly decreased damage depth into an alloy substrate, even under the thermal cycle condition as compared with that of the uncoated Inconel X750 (BX). In general, the C₂S-CZ-TBC system is subjected to more significant thickness loss in the top coat layer than the YSZ system, regardless of the heat treatment condition and the chromium content of the bond coat. In particular, the fact that such a top coat thickness loss was more pronounced in the isothermal condition suggests that a constituent of the top coat is highly reactive with the molten salt environment.

In the hot corrosion test at temperatures higher than 900 °C, on the other hand, the highly reactive nature of the C₂S-CZ top coat led to the complete removal of the top coat layer. In the thermal cycle corrosion test, furthermore, almost all the coating layers disappeared, including a NiCrAlY bond coat, probably due to the combined damage of the reaction-enhanced spalling in the top coat and the cyclic and intensive corrosion attack of the bond coat. This brought about a markedly increased damage depth in the alloy substrate, as shown for the C₂S-CZ-TBC system at 900 and 1000 °C in Fig. 8. In this case, however, increasing the chromium content in the bond coat appears effective in inhibiting the corrosive attack toward the substrate.¹

For the YSZ-TBC system, on the contrary, the damage depth was restrained to a lower level, even at 1000 °C, due to the relatively persistent coating layers. In addition, the YSZ-TBC

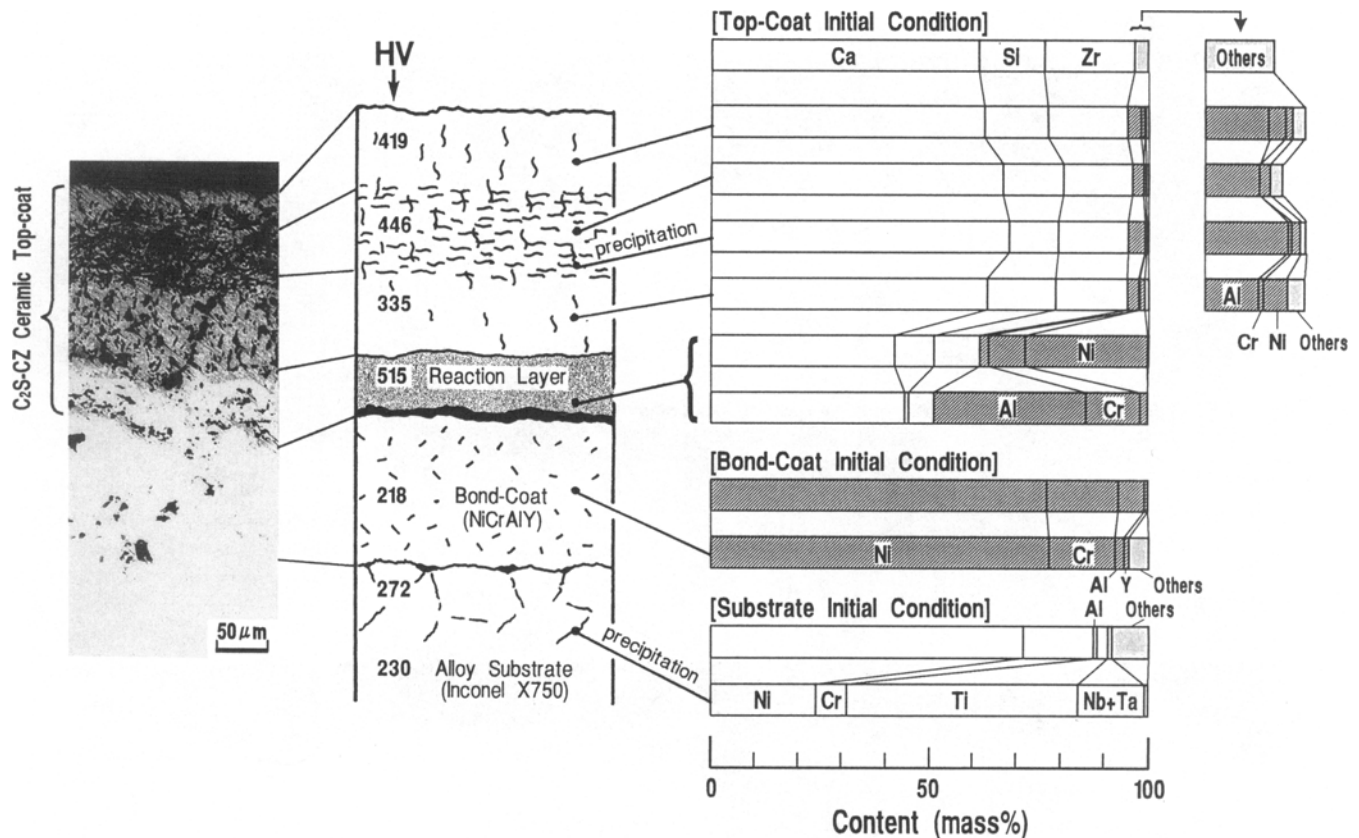


Fig. 6 Schematic illustration together with micrograph, EDX and Vickers microhardness distribution in the C₂S-CZ-TBC system after the isothermal oxidation test at 1100 °C for 100 h

system generally shows the same tendency as the case for high-temperature oxidation: air heat treatment (ZA) increases the thermal cycle sensitivity. As also for the YSZ-TBC system, increasing the chromium content in the bond coat results in a lower damage depth, as shown for HZV in Fig. 8.

3.2.2 Microstructural Features of Corrosion-Induced Failure

Metallographic examination has revealed that the corrosive failure morphology of each TBC system is essentially similar to that in high-temperature oxidation, as shown in Fig. 5, except for the case of the C₂S-CZ system at temperatures higher than 900 °C. The corrosive damage for the YSZ system was initially limited to the top coat/bond coat interface, where sulfidation and oxidation took place along the penetrating top coat crack. Thereafter, hot corrosion propagated progressively from the bond coat to the alloy substrate. Yoshida (Ref 9) has already clarified that hot corrosion in plasma spray coating systems proceeds mainly by the successive sulfidation/oxidation mechanism in the bond coat as well as in the alloy substrate, usually involving the formation of the low-melting Ni-Ni₃S₂ eutectic.

For the C₂S-CZ-TBC system, on the other hand, at the relatively lower temperature up to 800 °C, the interfacial corrosion between the top coat and bond coat is effectively restrained due

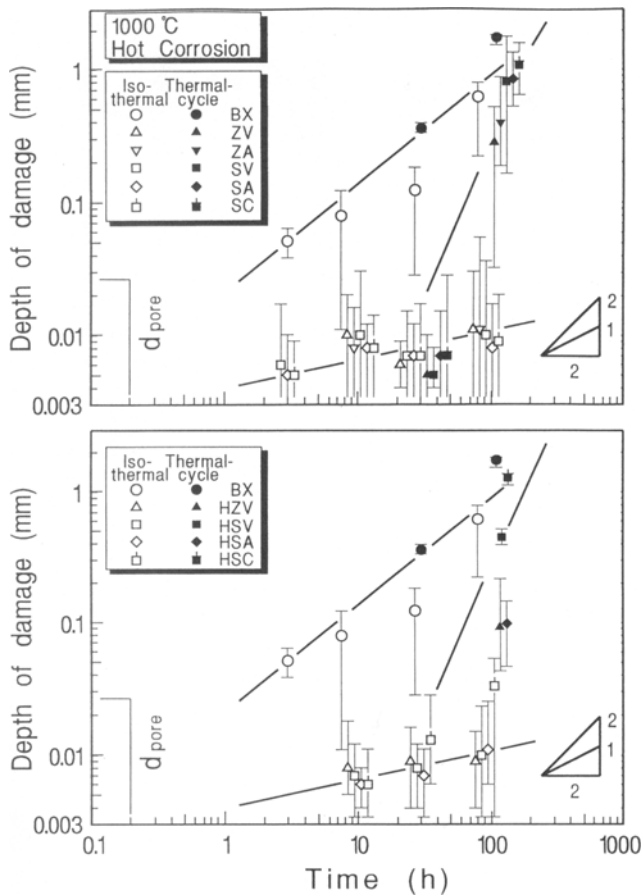


Fig. 7 Hot corrosion kinetics in terms of the damage depth for different TBC systems at 1000 °C for 100 h under isothermal and thermal cycle conditions

to development of the premature reaction layer. Instead, the top coat is subject to compositional and, therefore, microstructural modification by oxidation and/or sulfidation. This results in exacerbated spalling and, eventually, in corrosion of the bond coat. Figure 9 shows the backscattered electron and characteristic x-ray images at the cross-sectional surface zone of a C₂S-CZ-TBC system that was corrosion tested at 800 °C and simultaneously subjected to creep stress at 400 N/mm² for 336 h. It has been confirmed that no penetrating top coat crack is generated at all without the creep stress. It is evident that constituents of the top coat, such as calcium and silicon, are very reactive with the molten salt environment. For example, XRD analysis revealed that CaSO₄ was formed (Ref 10). Furthermore, there was little evidence that intensive corrosion attack was introduced along the top coat/bond coat interfacial region, in spite of the existence of vertical cracks through the top coat. This seems to be attributable to the protective effect of the reaction layer, which is mainly composed of aluminum- and chromium-rich oxides.

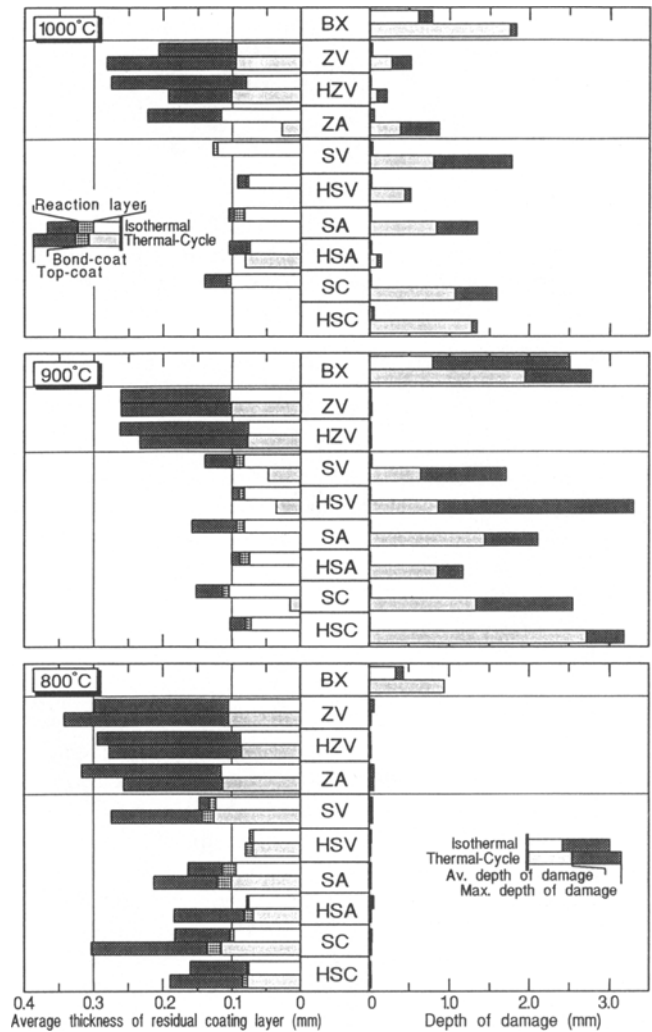


Fig. 8 Average thickness of the residual coating layer and the damage depth for different TBC systems after the hot corrosion test at various temperatures for 100 h under isothermal and thermal cycle conditions

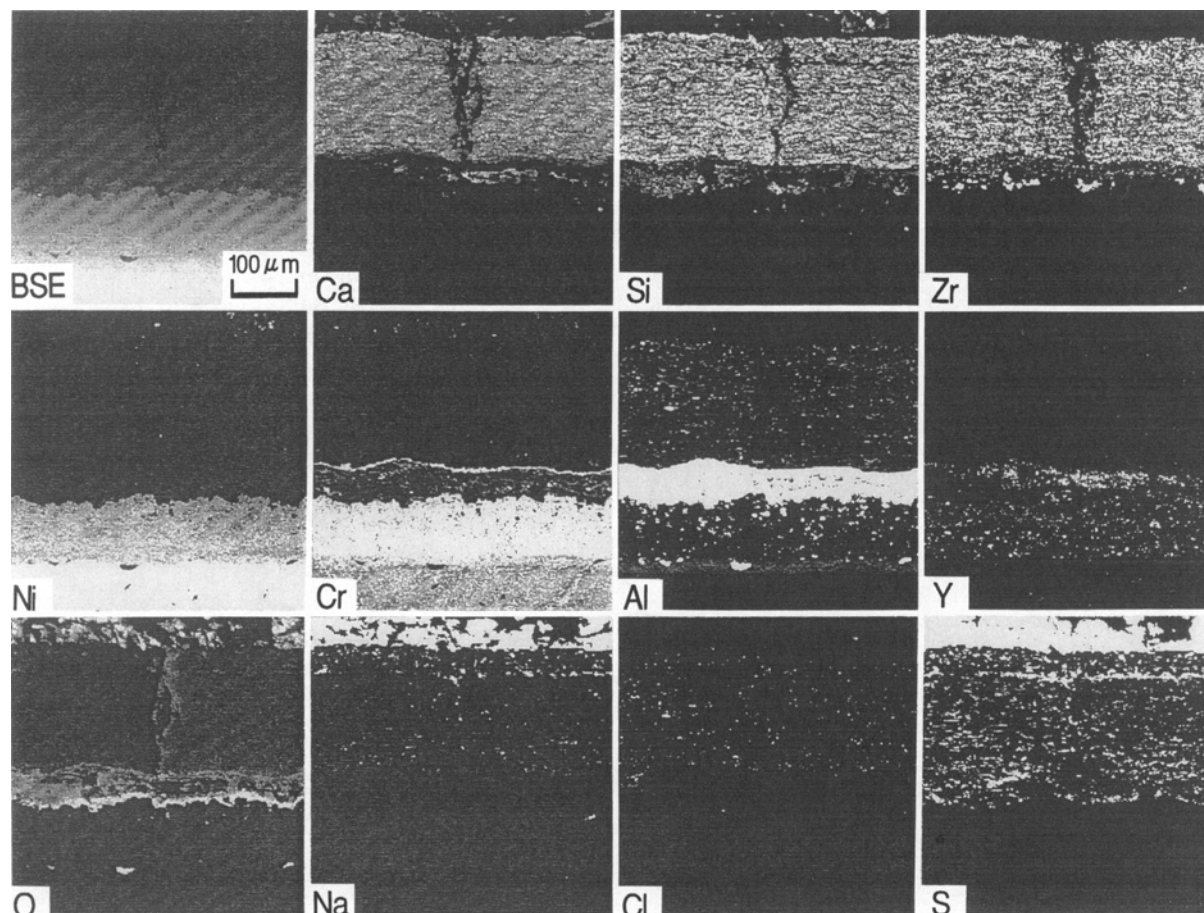


Fig. 9 Backscattered electron and characteristic x-ray images at the cross-sectional surface zone of the C₂S-CZ-TBC system, corrosion tested at 800 °C for 336 h under the creep stress of 400 N/mm².

However, the C₂S-CZ-TBC systems is subjected to more significant corrosive damage at temperatures higher than 900 °C, in which the corrosion-induced modification and, therefore, the surface recession take place very rapidly in the top coat.

4. Discussion

4.1 Classification of Failure Behavior in Different TBC Systems

On the basis of microstructural observations, including x-ray analyses such as EPMA and XRD, the failure behavior of the TBC systems subjected to high-temperature oxidation or hot corrosion can be classified into three types (Fig. 10). There is a distinct difference in coating failure behavior between the YSZ and C₂S-CZ systems. For the former, the penetrating top coat crack that preexists from the plasma processing and/or heat treatment process can be a critical defect for providing a short circuit path for the corrosive species, particularly in the case of hot corrosion. For the latter, on the contrary, such a macroscopic defect is essentially absent. Instead, an increased reactivity of the C₂S-CZ top coat is a life-limiting factor for the TBC system. Thus, the reaction layer developed at the inner region of the top coat appears to be both beneficial and harmful, depending on the

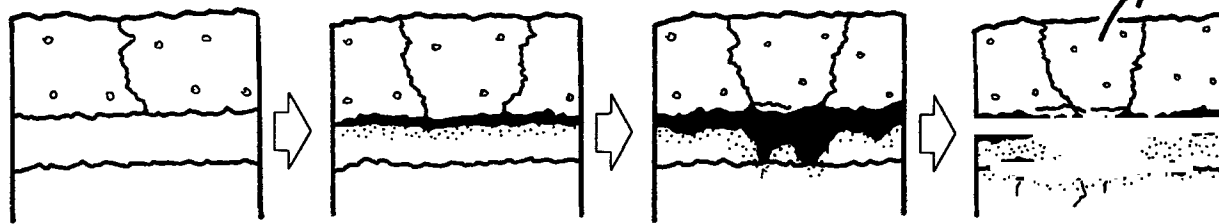
severity of the corrosive environment. In the less aggressive environment, such as for oxidation and lower-temperature hot corrosion (Type B in Fig. 10), the layer should be an effective barrier against the corrodant penetration; while in the highly aggressive environment (Type C), the reaction layer appears not only to lose the barrier function but also to permit rapid penetration of oxygen and/or sulfur toward the bond coat, at which both aluminum and chromium have been exhausted due to the reaction layer formation.

4.2 Effect of Coating Parameters on the Corrosive Failure Resistance of TBC Systems

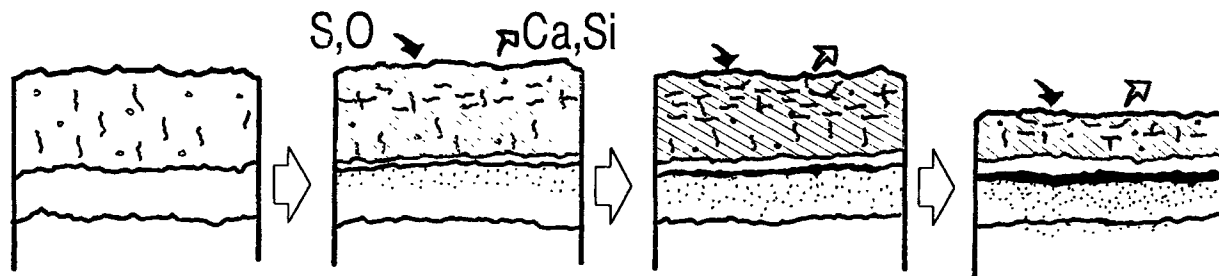
4.2.1 Effect of Heat Treatment

It is known that heat treatment after plasma spray coating is beneficial not only for recovering the strength properties of the alloy substrate but also for increasing the adhesion of the coating components to the alloy substrate. In this study, heat treatment was found to be effective to some degree for improving the coating adhesion, as can be seen in Fig. 4. Heat treatment also appeared to increase the suppression of the localized corrosive damage and subsequent spalling, mainly due to the enhanced homogenization of not only the metallic bond coat but also the ceramic top coat.

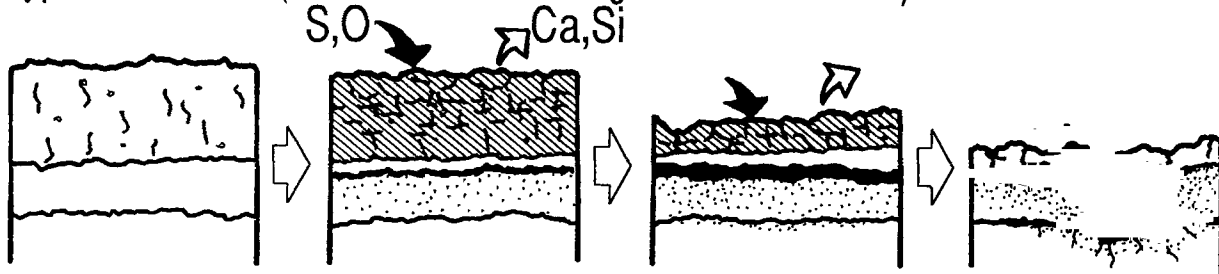
TypeA : YSZ (Oxidation and Hot Corrosion)



TypeB : C₂S-CZ (1100°C -Oxidation and 800°C -Hot Corrosion)



TypeC : C₂S-CZ (Hot Corrosion at Higher Than 900°C)



Stage I

Stage II

Stage III

Stage IV

Fig. 10 Schematic illustrations showing various stages of failure behavior in different TBC systems in high-temperature oxidation and hot corrosion

However, the atmosphere of the heat treatment, in particular of the solution treatment, should be one of the important factors for determining the environmental performance of the TBC system. For the YSZ-TBC system, for instance, heat treatment in air tends to cause enhanced interfacial oxidation along vertical cracks in the top coat, which result in premature top coat spallation compared with vacuum treated samples. It has been reported by Wu and Chang (Ref 11) that for the YSZ-TBC system, oxide growth at the top coat/bond coat interface promotes interfacial crack propagation and eventually causes significant failure for the TBC system under the thermal cycle condition.

For the C₂S-CZ-TBC system, conversely, the detrimental effect of the air treatment seems less pronounced, probably due to the dominatingly protective effect by the reaction layer.

4.2.2 Effect of Bond-Coat Constituents

For the YSZ-TBC system, an increased chromium content in the bond coat results in decreased damage depth, both in high-temperature oxidation and in hot corrosion. The reasons are increased protection of the bond coat itself with higher chromium content, and increased adhesion between the top coat and bond

coat. Stecura (Ref 12, 13) has reported that the spalling resistance of the top coat in the YSZ-TBC system depends strongly on the chromium content in the NiCrAlY bond coat. Then, the higher the chromium content in the bond coat, the more effectively the top coat spalling will be suppressed. In the present study, however, only the damage depth is reduced by increasing the chromium content, with little difference in the thickness of residual coating layer. Consequently, it is reasonable to consider that the effect of chromium is more significant for the corrosion resistance of the bond coat itself.

For the C₂S-CZ-TBC system, on the contrary, a different aspect of the chromium effect was obtained. In this case, the beneficial effect of increasing the chromium content depends strongly on both the environmental condition and the heat treatment. This is closely related to the character of the reaction layer involving chromium.

5. Conclusions

Quantitative evaluation of the thermochemical resistance and coating failure analysis of high-temperature oxidation and

hot corrosion tests were made for two TBC systems, YSZ and C₂S-CZ, with different coating parameters such as the heat treatment conditions and the chromium content of the NiCrAlY bond coat. The principal results obtained are as follows:

- In the high-temperature oxidation up to 1100 °C, the C₂S-CZ systems showed generally good coating adhesion compared to the YSZ systems. An advantage of the C₂S-CZ system was more pronounced in the thermal cycle oxidation. Coating failure in the YSZ system was caused by extensive exfoliation of the top coat, which was enhanced by the preferential oxidation along the top coat/bond coat interface through vertical cracks in the top coat. On the other hand, the nature of the coating layer in the C₂S-CZ system was found to be modified by the increased reactivity with oxygen, by which a reaction layer was developed at the inner region of the top coat that increased the spalling resistance.
- In the hot corrosion tests up to 1000 °C, constituents of the top coat, such as calcium and silicon in the C₂S-CZ system, were more reactive with the molten salt environment, so that the top coat became rapidly unstable and lost its protective function. Conversely, the failure behavior of the YSZ system subjected to hot corrosion was essentially similar to that in high-temperature oxidation, in which the top coat remained relatively stable.
- The atmospheric condition of the heat treatment, in particular the solution treatment, was found to alter the corrosion performance of the TBC systems. In general, heat treatment in air was harmful for the YSZ system because it exacerbated interfacial oxidation, which induced extensive top coat spalling, particularly under the thermal cycle condition. For the C₂S-CZ system, conversely, the coating performance had less atmospheric sensitivity with respect to heat treatment.
- The reaction layer developed in the heat treatment, high-temperature oxidation and hot corrosion of the C₂S-CZ systems was characterized and its effect on the thermochemical performance of the TBC system was briefly discussed.

Acknowledgments

The authors wish to acknowledge Mr. J. Takeuchi and his co-workers at Tocalo Co., Ltd., for supplying the TBC specimens, and JEOL for valuable analytic data of EPMA. The experimental work in this study was competently carried out by H. Sone,

who was an undergraduate student at Tokyo Metropolitan University.

References

1. G.W. Meetham, Coating Requirements in Gas Turbine Engines, *J. Vac. Sci. Technol.*, Vol A3 (No. 6), 1985, p 2509-2515
2. H. Takeda, *Ceramic Coating*, H. Takeda, Ed., Nikkan-Kogyo-Shimbunsha, Tokyo, 1988, p 179-199 (in Japanese)
3. S.R.J. Saunders and J.R. Nicholls, Coatings and Surface Treatments for High Temperature Oxidation Resistance, *Mater. Sci. Technol.*, Vol 5, 1989, p 780-798
4. S. Sodeoka, M. Suzuki, T. Inoue, Y. Ono, and K. Ueno, Plasma Spray under Controlled Atmosphere up to 300 kPa, *Proc. ITSC '95*, A. Ohmori, Ed., High Temp. Soc. Japan, Vol 1, 1995, p 283-288
5. P.E. Hodge, R.A. Miller, and M.A. Gedwill, Evaluation of the Hot Corrosion Behavior of Thermal Barrier Coatings, *Thin Solid Films*, Vol 73, 1990, p 447-453
6. R. Tanaka and O. Miyagawa, Test Methods for Fuel Oil Ash Corrosion of Heat Resisting Alloys, *Trans. ASME-JEMT*, Vol 10, 1973, p 322-329
7. M. Yoshida, O. Miyagawa, H. Mizuno, and H. Fujishiro, Effect of Environmental Factors on the Creep Rupture Properties of a Nickel-Base Superalloy Subjected to Hot Corrosion, *Trans. Japan Inst. Metals*, Vol 29, 1988, p 26-41
8. K. Wada, M. Yoshida, and Y. Harada, Failure and Strength Degradation in Hot Corrosion Environment of Various Nickel-Base Superalloy/Coating Systems by Plasma Spraying, *Rep. 123rd Committee of Japan Soc. Promotion Sci.*, Vol 32, 1991, p 405-425 (in Japanese)
9. M. Yoshida, Effect of Hot Corrosion on the Mechanical Performances of Superalloys and Coating Systems, *Corros. Sci.*, Vol 35, 1993, p 1115-1124
10. M. Yoshida, T. Aranami, H. Taira, and Y. Harada, Failure Analysis of Some Plasma Spray Coated Superalloy Systems Subjected to the Synergistic High Temperature Damage in Actual Gas Turbine or in Laboratory, *Proc. ITSC '95*, A. Ohmori, Ed., High Temp. Soc. Japan, Vol 1, 1995, p 89-94
11. B.C. Wu and E. Chang, Thermal Cyclic Response of Yttria-Stabilized Zirconia/CoNiCrAlY Thermal Barrier Coatings, *Thin Solid Films*, Vol 172, 1989, p 185-196
12. S. Stecura, Effects of Yttrium, Aluminum and Chromium Concentrations in Bond Coatings on the Performance of Zirconia-Yttria Thermal Barriers, *Thin Solid Films*, Vol 73, 1980, p 481-489
13. S. Stecura, Two-Layer Thermal Barrier Coatings, Part I: Effects of Composition and Temperature on Oxidation Behavior and Failure, *Thin Solid Films*, Vol 182, 1989, p 121-139